Electronic Supplementary Material (ESI) for Journal of Materials Chemistry C.

Supporting Information

Efficient Narrowband Electroluminescence based on a Hetero-Bichromophore Thermally Activated Delayed Fluorescence Dyad

You-Jun Yu[#], Sheng-Nan Zou[#], Chen-Chen Peng, Zi-Qi Feng, Yang-Kun Qu, Sheng-Yi Yang, Zuo-Quan Jiang*, Liang-Sheng Liao*

Institute of Functional Nano & Soft Materials (FUNSOM), Jiangsu Key Laboratory for Carbon-Based Functional Materials & Devices, Soochow University, 199 Ren'ai Road, Suzhou, 215123, Jiangsu, PR China
E-mail: zqjiang@suda.edu.cn; lsliao@suda.edu.cn

[#] These authors contributed equally.

Content

1 Experimental Section

1.1 General experimental methods

The raw reagents, catalysts, and chemicals involved in the initial reaction were all from commercial companies and without further purification. Solvents used in the reaction, such as toluene, tetrahydrofuran, etc. were purified by the solvents purification system. ^{1}H NMR and ^{13}C NMR spectra were recorded on a Bruker 400 spectrometer or Bruker 600 spectrometer at room temperature. Mass spectra and time of Flight MS-MALDI (MALDI-TOF) were performed on a Thermo ISQ mass spectrometer using a direct exposure probe and Bruker Autoflex II/Compass 1.0, respectively. The ultraviolet−visible (UV−vis) absorption spectra were measured by a Shimadzu UV-2600 spectrophotometer. Fluorescent, as well as phosphorescent spectra, were measured by a Hitachi F-4600 spectrophotometer. Thermogravimetric analysis (TGA) was measured by a METTLER TOLEDO TGA1 under a high purity nitrogen atmosphere. The temperature was increased to 700 ^{o}C with a heating rate of 10 ^{o}C/minute. DFT and TD-DFT calculations were performed utilizing B3LYP with the 6-31g(d) atomic basis set.[1]. Electrochemical analysis was achieved on a CHI 600D electrochemical workstation, and the scan rate was 100 mV S^{-1} at room temperature. The three-electrode configuration system in n-Bu$_4$NPF$_6$ (0.1 M) DMF solution. The redox potential of ferrocene/ferrocenium(Fc/Fc$^+$) was measured under room temperature (for calibration). The PLQY was measured using Hamamatsu C9920-02G in nitrogen or air atmosphere. Transient spectra were obtained by using the Quantaurus-Tau fluorescence lifetime measurement system (C11367-03, Hamamatsu Photonics Co.) in a vacuum.

1.2 Single crystal information

The crystal BO-QAO was grown by slow evaporation in dichloromethane and tetrahydrofuran. We use Bruker D8-Venture diffractometer with a Turbo X-ray Source (Mo–Kα radiation, $\lambda = 0.71073$ Å) adopting the direct-drive rotating anode technique and a CMOS detector to collect the single-crystal data. The structures were solved by direct methods and refined by the full-matrix least-squares on F2 using the SHELXTL-2014 program. The X-ray crystallographic coordinates for the structure reported in this study have been deposited at the Cambridge Crystallographic Data Centre (CCDC), under deposition number

BOQAO (2057629). These data can be obtained free of charge from The Cambridge Crystallographic Data Centre "http://www.ccdc.cam.ac.uk/data request/cif".

1.3 Device fabrication process

OLEDs were fabricated on the ITO glass substrates layer (110 nm, 15 Ω/square) under a base pressure of 3 × 10^{-6} Torr. The active area of each device is 0.09 cm^2. Deposition rates and thicknesses of all materials were monitored with oscillating quartz crystals. The doping layer was deposited by utilizing two different sensors to monitor the deposition rates of both host material and dopant material. The deposition rate of the host was controlled at 0.2 nm s^{-1}, and the deposition rate of the dopant was adjusted according to the volume ratio doped in the host materials. The electroluminescence (EL) and current density-voltage(*J-V*) characteristics of the devices were measured by a constant current source (Keithley 2400 SourceMeter) combined with a photometer (Photo Research SpectraScan PR655).

1.4 Thermal properties

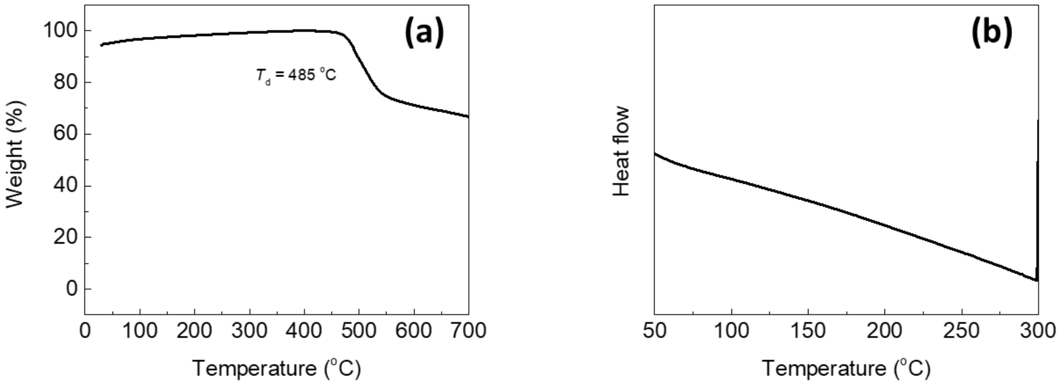

Fig. S1. (a) Thermogravimetric analysis (TGA) and (b) differential scanning calorimetry (DSC) curves of **BOQAO**.

1.5 Simulation results

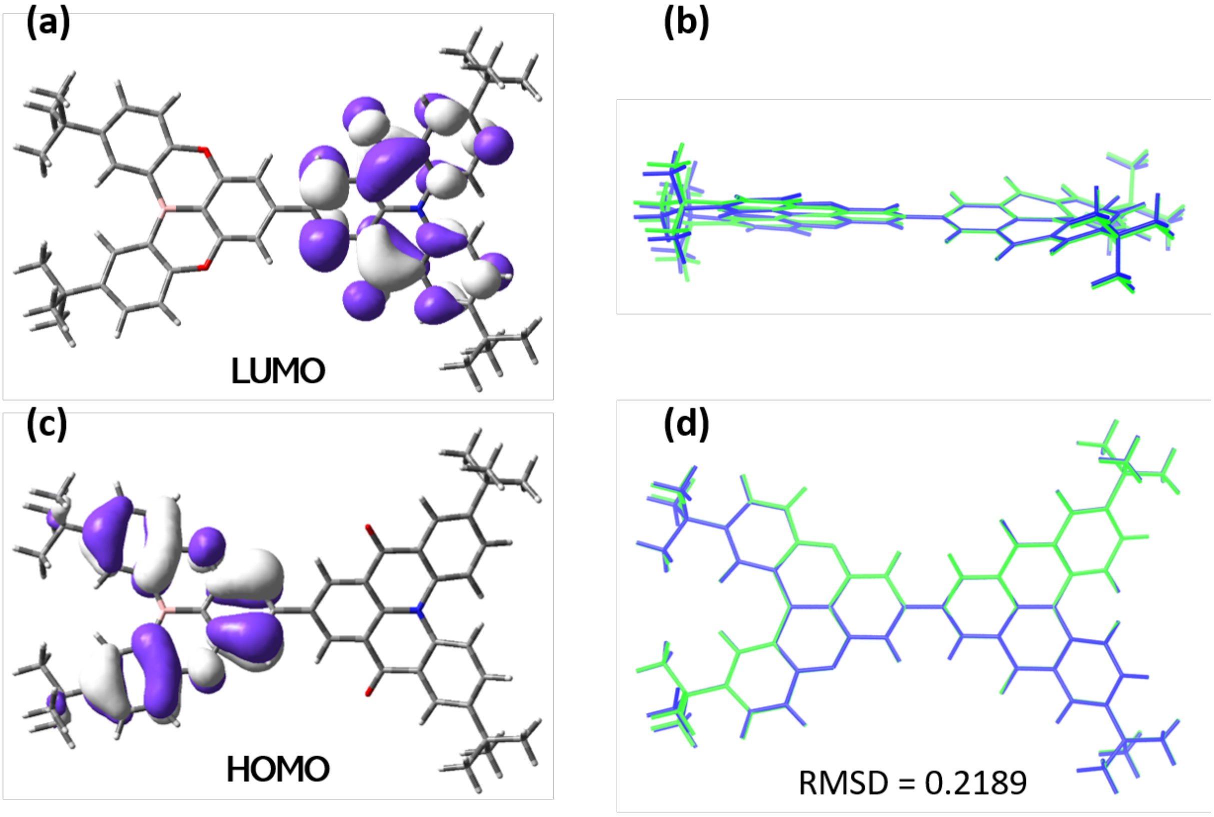

Fig. S2. Simulation results for BOQAO. (c) HOMO and (a) LUMO distributions of BOQAO. (b) (d) The geometric difference between the S_0 (blue) and S_1 (green) configurations. The Root mean square displacement/deviation (RMSD) value between the two configurations is 0.2189.

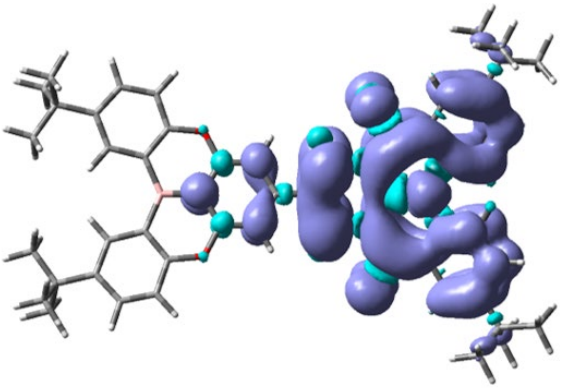

Fig. S3. triplet spin density distribution of **BOQAO**.

1.6 Electrochemical properties

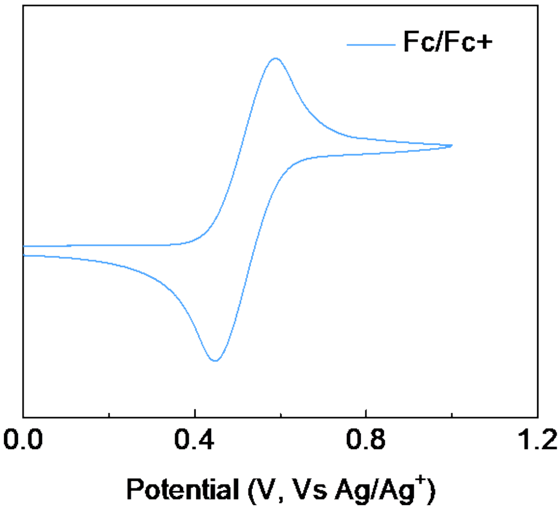

Fig. S4. CV curves of Ferrocene.

1.7 photophysical properties

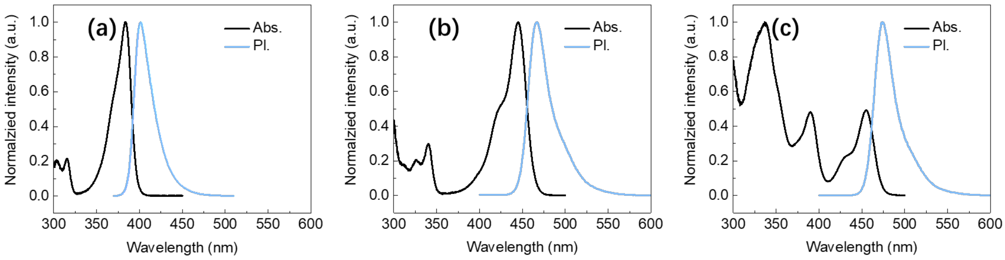

Fig. S5. Absorption spectra of (a) **tBuBO**, (b) **tBuQAO**, and (c) **BOQAO**.

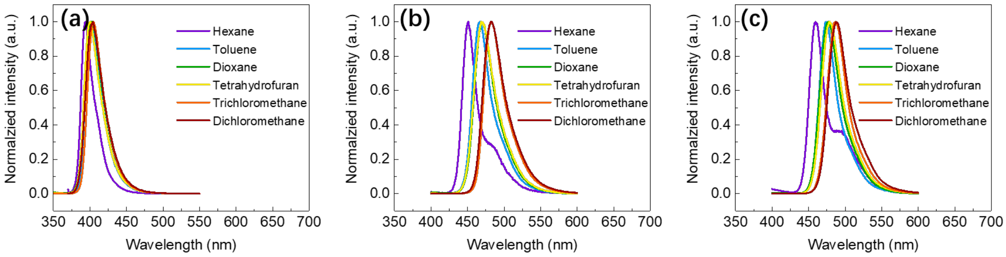

Fig. S6. Fluorescence spectra of (a) **tBuBO**, (b) **tBuQAO**, and (c) **BOQAO** in different solvents.

Table S1. Photophysical properties of **tBuBO**, **tBuQAO**, and **BOQAO**

Solvent	**tBuBO**		**tBuQAO**		**BOQAO**	
	$\lambda_{\mathrm{Fl.}}$ nm	FWHM nm	$\lambda_{\mathrm{Fl.}}$ nm	FWHM nm	$\lambda_{\mathrm{Fl.}}$ nm	FWHM nm
hexane	394	21	451	22	460	22
toluene	401	24	467	30	474	30
dioxane	402	29	469	32	477	32
tetrahydrofuran	400	26	469	35	479	35
trichloromethane	405	26	483	32	487	32
dichloromethane	404	28	482	36	488	36

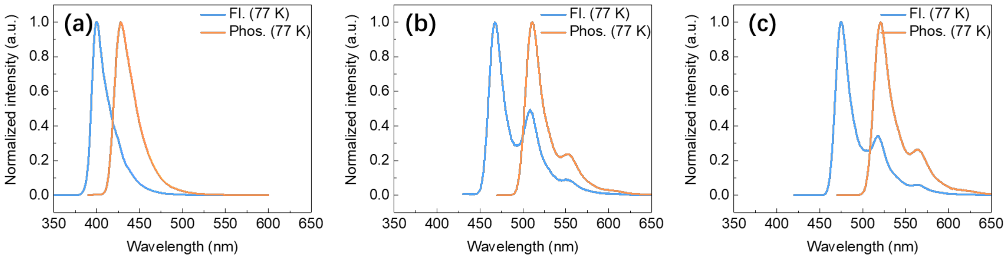

Fig. S7. Fluorescence and phosphorescence spectra of (a) **tBuBO**, (b) **tBuQAO**, and (c) **BOQAO**.

Table S2. Photophysical properties of **tBuBO**, **tBuQAO**, and **BOQAO**

	$\lambda_{\mathrm{abs.}}$[a] nm	$\lambda_{\mathrm{Fl.}}$[a] nm	HOMO[b] eV	LUMO[b] eV	E_g[c] eV	S_1[d] eV	T_1[e] eV	ΔE_{ST}[f] eV
tBuBO	303, 316, 384	401	-5.80	-2.80	3.00	3.19	3.00	0.19
tBuQAO	326, 341, 445	467	-5.85	-3.00	2.85	2.73	2.51	0.22
BOQAO	337, 390, 455	474	-5.77	-3.06	2.71	2.68	2.46	0.22

[a] Measured in dilute toluene solution (10^{-5} M) at room temperature. [b] Evaluated from the CV curves. [c] E_g = LUMO – HOMO. [d] Evaluated from the onset of the fluorescence spectra (measured in dilute toluene at 77 K). [e] Evaluated from the onset of the phosphorescence spectra (measured in dilute toluene at 77 K). [f] $\Delta E_{\mathrm{ST}} = S_1 - T_1$.

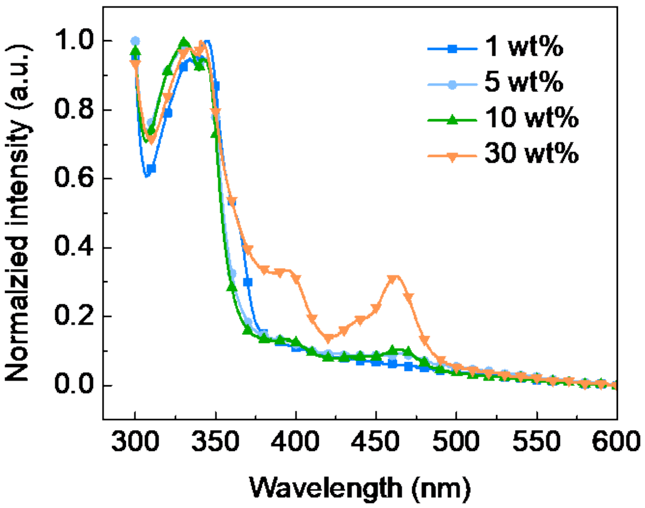

Fig. S8. Absorption spectra of BOQAO in CBP with different doping ratios.

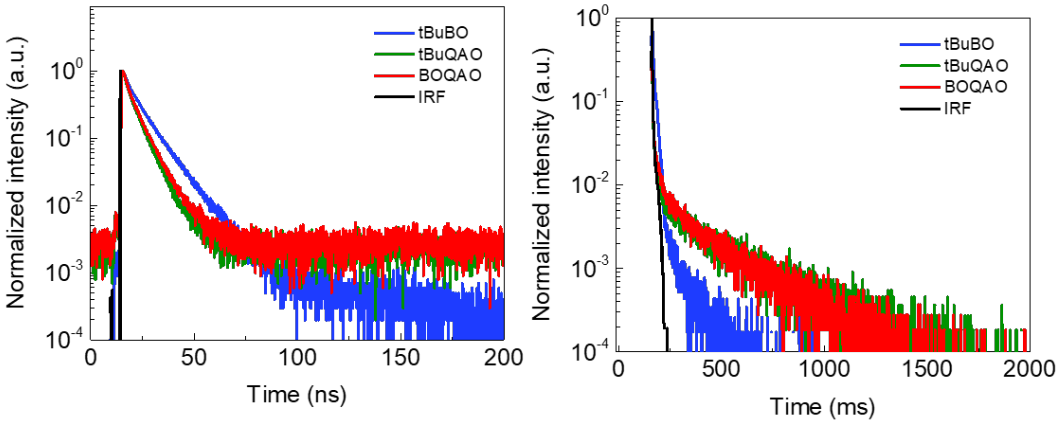

Fig. S9 Transient spectra of 5wt% tBuBO, tBuQAO, and BOQAO in CBP.

Table S3 Photophysical properties of tBuBO, tBuQAO, and BOQAO in doped CBP film (5wt%)

	λ^a nm	PLQY^b (Total/PF/DF) %	$\tau_{PF}/\tau_{DF}{}^c$ ns/μs
tBuBO	408	97.0/60.5/36.5	10/59
tBuQAO	479	93.1/11.6/81.5	6/255
BOQAO	487	98.7/19.0/79.7	6/214

[a]Emission peak of the corresponding emitter in doped CBP film (5 wt%); [b]Measured under N_2 atmosphere and the excitation wavelength is 310 nm; [c]Measured in a vacuum.

For a TADF system, the main exciton loss channels are either singlet or triplet nonradiative transition processes. Owing to extremely high values of PLQYs, the singlet nonradiative transition process (k_{nr}^{S}) can thus be ignored and all exciton loss can thus be attributed to the triplet nonradiative transition process (k_{nr}^{T}). The key kinetic parameters of the three emitters are estimated according to the following equations[2,7] and the key kinetic parameters are summarized in Table S4.

$$k_{PF} = \frac{1}{\tau_{PF}}$$

$$k_{DF} = \frac{1}{\tau_{DF}}$$

$$k_{r}^{S} = k_{PF}\phi_{PF}$$

$$k_{ISC} = k_{PF}(1 - \phi_{PF})$$

$$k_{RISC} = \frac{k_{PF} \times k_{DF} \times \phi_{DF}}{k_{ISC} \times \phi_{PF}}$$

$$k_{nr}^{T} = k_{DF} - \left(1 - \frac{k_{ISC}}{k_{PF}}\right) \times k_{RISC}$$

Table S4 Photophysical properties of tBuBO, tBuQAO, and BOQAO in doped CBP film (5wt%)

	k_{PF} S^{-1}	k_{DF} S^{-1}	k_{r}^{S} S^{-1}	k_{ISC} S^{-1}	k_{RISC} S^{-1}	k_{nr}^{T} S^{-1}
tBuBO	1.0×10^{8}	16.9×10^{3}	6.0×10^{7}	0.4×10^{8}	2.6×10^{4}	1.3×10^{3}
tBuQAO	1.7×10^{8}	3.9×10^{3}	1.9×10^{7}	1.5×10^{8}	3.1×10^{4}	3.1×10^{2}
BOQAO	1.7×10^{8}	4.7×10^{3}	3.2×10^{7}	1.3×10^{8}	2.4×10^{4}	7.5×10^{1}

k_{PF} and k_{DF} are the radiative rate constants for prompt and delayed components, respectively; k_{r}^{S} and k_{nr}^{T} are the rate constants of singlet radiative transition and triplet nonradiative transition; k_{ISC} and k_{RISC} are the rate constants for ISC and RISC, respectively.

1.8 Crystal data and structure refinement

Table S3. Crystal data and structure refinement for BOQAO.

Empirical formula	$C_{54}H_{52}BNO_4$
Formula weight	789.40
Temperature/K	170.0
Crystal system	triclinic
Space group	P-1
Unit cell dimensions	12.6019(7) 14.6860(8) 15.0625(9) α/°: 77.047(2) β/°: 68.664(2) γ/°: 66.920(2)
Volume/ Å^3	2377.9(2)
Z	2
Density/g/cm^3	1.222 (calculated)
Absorption coefficient/mm^{-1}	0.183
F(000)	924.0
Crystal size/mm^3	0.15 × 0.08 × 0.03
Radiation	MoKα (λ = 0.71073)
Theta range for data collection/°	3.894 to 52.836
Index ranges	$-15 \leq h \leq 14, -18 \leq k \leq 17, -18 \leq l \leq 18$
Reflections collected	27099
Independent reflections	9651 [R_{int} = 0.0772, R_{sigma} = 0.1090]
Data/restraints/parameters	9651/0/580
Goodness-of-fit on F^2	1.018
Final R indices [I>2sigma(I)]	R_1 = 0.0709, wR_2 = 0.1428
R indices (all data)	R_1 = 0.1601, wR_2 = 0.1939
Largest diff. peak and hole	0.43/-0.52
CCDC number	2057629

1.9 device performance

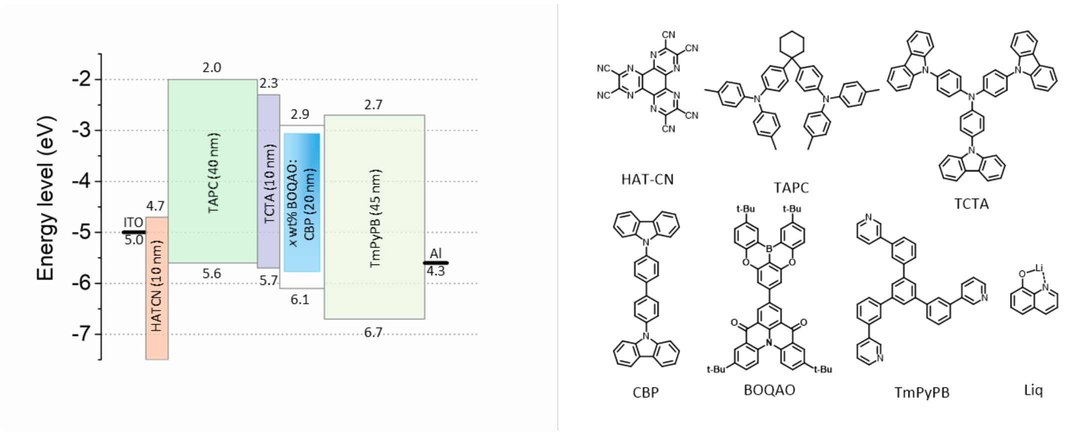

Fig. S10 Energy-level diagram and chemical structures of the materials for the OLEDs based on **BOQAO** as MR-TADF emitters.

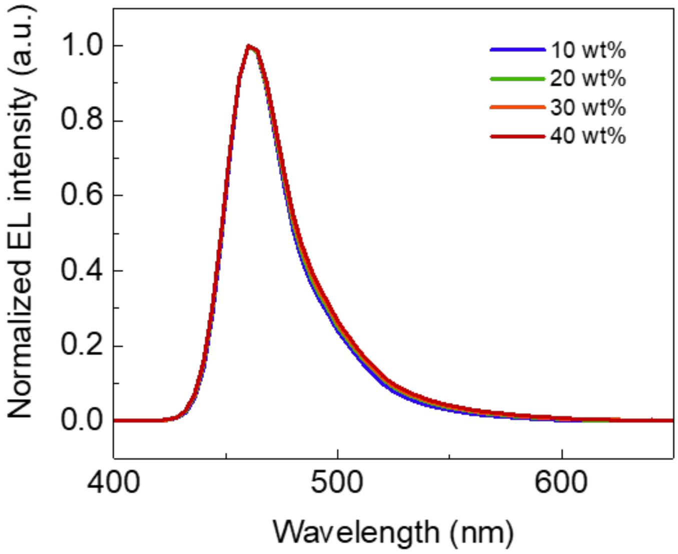

Fig. S11 Normalized Electroluminescence spectra of OLED devices based on BOQAO.

Table S4. Key parameters of reported OLED device based on QAO derivatives

Name	Doping ratio wt%	Host	λ_{EL} nm	FWHM nm	CIE (x, y)	EQE %	Ref.
QAO	5	mCP	468	39	(0.13, 0.18)	19.4	3
QAO-DAd	5	CBP	552	- -	(0.41,0.56)	23.9	
3-PhQAD	2	mCP	480	44	(0.13, 0.32)	19.1	4
7-PhQAD	2	mCP	472	37	(0.12, 0.24)	18.7	
DDiKTa	9	DPEPO	500	59	(0.18, 0.53)	19.0	5
DQAO	8	mCP	472	34	(0.12, 0.18)	15.2	6
OQAO	5	CBP	532	45	(0.32, 0.65)	20.3	
SQAO	1	mCPCN	564	72	(0.47, 0.52)	17.8	
QAD-Cz	1	mCP	494	57	(0.16,0.47)	20.3	7
QAD-2Cz	12	mCP	530	56	(0.30,0.65)	27.3	
QAD-mTDPA	1.5	CBP	589	67	(0.55,0.44)	26.3	
QA-2	3	PPCz	463	37	(0.13, 0.14)	19.0	8
QA-PF	3	mCP	474	27	(0.12,0.17)	16.8	9
QA-PCN	3	mCP	473	30	(0.12,0.18)	16.9	
QA-PMO	3	mCP	484	27	(0.11,0.30)	15.0	
QA-PCZ	3	mCP	482	29	(0.11,0.28)	17.5	
1	3	mCBP	-	-	(0.23, 0.59)	14	10
2	3	mCBP	-	-	(0.41, 0.56)	16	
3	3	mCBP	-	-	(0.46, 0.54)	10	
4	3	mCBP	-	-	(0.54, 0.45)	1	
5	3	mCBP	-	-	(0.57, 0.43)	2	
QAO-PhCz	5	mCBP	470	36	(0.13, 0.18)	12.4	11
BOQAO	5	CBP	484	32	(0.11, 0.37)	21.8	This work

1.10 Synthesis

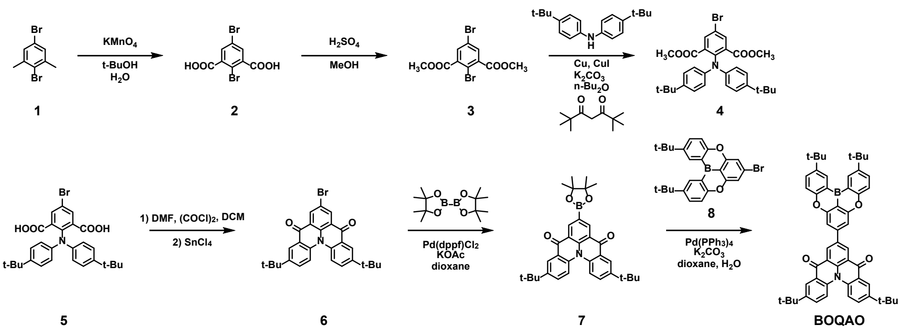

Scheme S1. Synthetic route for **BO-QAO**.

Intermediate 3 was synthesized according to the literature procedures.[12] All other reagents and solvents are used from commercial sources without further purification.

Synthesis of 2-(bis(4-(tert-butyl)phenyl)amino)-5-bromoisophthalate (4).

Compound dimethyl 2-bromoisophthalate (3) (7.04 g, 20 mmol), bis(4-(tert-butyl)phenyl)amine (5.63 g, 20 mmol), potassium carbonate (4.15 g, 30 mmol), copper(I) iodide (0.38 g, 2 mmol), 2,2,6,6-tetramethylheptane-3,5-dione (0.37 g, 2 mmol), and activated copper powder (0.13 g, 2 mmol) were combined with 150 mL 1-butoxybutane in a round bottom flask equipped with a reflux condenser and magnetic stir bar. The reaction mixture was heated to 160 °C for 48 h under argon. After cooled to room temperature, the reaction was filtered, the solvent removed under vacuum condition, and then the residue purified by column chromatography on silica gel using petroleum ether/dichloromethane (1/1, v/v) as eluent, yellow solid was finally obtained. Yield: 5.64 g (51%). ^{1}H NMR (400 MHz, DMSO-d6) δ 7.85 (s, 2H), 7.21 (d, J = 8.7 Hz, 4H), 6.73 (d, J = 8.7 Hz, 4H), 3.32 (s, 18H), 3.28 (s, 6H). ^{13}C NMR (101 MHz, DMSO-d6) δ 164.30, 143.60, 142.62, 141.71, 134.22, 132.95, 124.46, 120.69, 115.66, 51.06, 32.92, 30.13. MS (EI) m/z: 551.174 [M$^+$]. Calcd for $C_{30}H_{34}BrNO_4$: 551.167.

Synthesis of 2-(bis(4-(tert-butyl)phenyl)amino)-5-bromoisophthalic acid (5).

Compound 4 (5.50 g, 9.95 mmol) and sodium hydroxide (1.99 g, 49.77 mmol) in a solution of 100 mL EtOH/water (1/1, v/v) heated to reflux for 48 h. Acidification with concentrated hydrochloric acid precipitated the triarylamine diacid, which was collected by vacuum filtration and oven-dried (80 °C) overnight, then employed directly without further purification. Yield: 4.80 g (92.0%).

Synthesis of 7-bromo-3,11-di-tert-butylquinolino[3,2,1-de]acridine-5,9-dione (6).

Compound 5 (3.00 g, 5.72 mmol) was dispersed in dry dichloromethane (60 mL) in a three-neck round-bottom flask equipped with a magnetic stir bar and reflux condenser with a drying tube. Two drops of N, N-dimethylformamide was added followed by oxalyl chloride (1.07 mL, 12.58 mmol). The reaction was heated to reflux for 0.5 h. Tin(IV) chloride (5.20 mL, 12.58 mmol) was added and the reaction refluxed for an additional 3 h. The reaction mixture was added dropwise to an aqueous solution of sodium hydroxide (≈ 1 M) and extracted with dichloromethane. The organic layer dried over sodium sulfate and concentrated. The crude product was then purified by flash chromatography using dichloromethane/petroleum ether (3/1, v/v) as the eluent to give a bright yellow-green solid. Yield: 1.79 g (64.0%). ^{1}H NMR (400 MHz, Chloroform-d) δ 8.90 – 8.69 (m, 2H), 8.44 (q, *J* = 1.8 Hz, 2H), 8.06 (dt, *J* = 8.9, 1.5 Hz, 2H), 7.73 (dt, *J* = 9.0, 1.7 Hz, 2H), 1.43 (s, 18H). ^{13}C NMR (101 MHz, $CDCl_3$) δ 177.73, 148.75, 137.58, 137.51, 135.03, 130.79, 125.77, 124.93, 123.83, 120.19, 117.02, 34.88, 31.21. MS (EI) m/z: 487.337 [M+]. Calcd. for $C_{28}H_{26}BrNO_2$: 487.115.

Synthesis of 3,11-di-tert-butyl-7-(4,4,5,5-tetramethyl-1,3,2-dioxaborolan-2-yl)quinolino[3,2,1-de]acridine-5,9-dione (7).

Compound dimethyl 5-bromo-2-(di([1,1'-biphenyl]-4-yl)amino)isophthalate (2) (1.5 g, 3.07 mmol), 4,4,4',4',5,5,5',5'-octamethyl-2,2'-bi(1,3,2-dioxaborolane) (1.09 g, 4.30 mmol), Pd(dppf)Cl_2 (125 mg, 0.15 mmol) and potassium acetate (1.21 g, 12.28 mmol) were combined with 30 mL 1,4-dioxane in a round bottom flask equipped with a reflux condenser and magnetic stir bar. The reaction mixture was heated to 100 °C for 12 h under argon. After cooled to room temperature, the reaction was filtered, the solvent removed under vacuum condition, and then the residue purified by column chromatography on silica gel using petroleum ether/dichloromethane (1/2, v/v) as eluent, yellow solid was finally obtained. Yield: 1.38 g (84%). ^{1}H NMR (400 MHz, Chloroform-d) δ 9.15 (s, 2H), 8.48 (d, *J* = 2.5 Hz, 2H), 8.09 (d, *J* = 8.9 Hz, 2H), 7.73 (dd, *J* = 8.9, 2.5 Hz, 2H), 1.45 (s, 18H), 1.40 (s, 12H). ^{13}C NMR (101 MHz, Chloroform-d) δ 178.88, 148.43, 140.55, 139.39, 137.54, 130.30, 126.22, 123.73, 122.60, 120.16, 84.39, 34.85, 31.26, 24.94. MS (EI) m/z: 535.275 [M+]. Calcd for $C_{34}H_{38}BNO_4$: 535.289.

Synthesis of BOQAO

3,11-di-tert-butyl-7-(4,4,5,5-tetramethyl-1,3,2-dioxaborolan-2-yl)quinolino[3,2,1-de]acridine-5,9-dione (7) (1.28 g, 2.39 mmol), 7-bromo-2,12-di-tert-butyl-5,9-dioxa-13b-boranaphtho[3,2,1-*de*]anthracene (8) (1.00 g, 2.17 mmol), tetrakis(triphenylphosphine)palladium (250.56 mg, 0.22 mmol) and potassium carbonate (1.20 g, 8.67 mmol) were combined with 50 mL 1,4-dioxane an 10 ml H_2O in a round bottom flask equipped with a reflux condenser and magnetic stir bar. The reaction mixture was heated to 100 °C for 10 h under argon. After cooled to room temperature, the reaction was filtered, the solvent removed under vacuum condition, and then the residue purified by column chromatography on silica gel using petroleum ether/dichloromethane (1/1, v/v) as eluent, yellow solid was finally obtained. Yield: 1.28 g (76%). ^{1}H NMR (400 MHz, Chloroform-d) δ 9.15 (s, 2H), 8.78 (d, *J* = 2.5 Hz, 2H), 8.53 (d, *J* = 2.4 Hz, 2H), 8.12 (d, *J* = 8.9 Hz, 2H), 7.78 (ddd, *J* = 18.9, 8.9, 2.4 Hz, 4H), 7.67 (s, 2H), 7.55 (d, *J* = 8.7 Hz, 2H), 1.51 (s, 18H), 1.47 (s, 18H). ^{13}C NMR (101 MHz, Chloroform-d) δ 178.77, 158.83, 158.12, 148.54, 145.09, 144.80, 138.61, 137.56, 135.41, 131.54, 131.25, 130.52, 130.24, 125.98, 123.94, 123.85, 121.82, 120.17, 118.10, 107.01, 34.89, 34.57, 31.57, 31.27. MS (EI) m/z: 789.423 [M^{+}]. Calcd for $C_{54}H_{52}BNO_4$: 789.399.

2 Reference

1. M. J. Frisch, G. W. Trucks, H. B. Schlegel, G. E. Scuseria, M. A. Robb, J. R. Cheeseman, G. Scalmani, V. Barone, B. Mennucci, G. A. Petersson, H. Nakatsuji, M. Caricato, X. Li, H. P. Hratchian, A. F. Izmaylov, J. Bloino, G. Zheng, J. L. Sonnenberg, M. Hada, M. Ehara, K. Toyota, R. Fukuda, J. Hasegawa, M. Ishida, T. Nakajima, Y. Honda, O. Kitao, H. Nakai, T. Vreven, J. A. Montgomery, Jr., J. E. Peralta, F. Ogliaro, M. Bearpark, J. J. Heyd, E. Brothers, K. N. Kudin, V. N. Staroverov, T. Keith, R. Kobayashi, J. Normand, K. Raghavachari, A. Rendell, J. C. Burant, S. S. Iyengar, J. Tomasi, M. Cossi, N. Rega, J. M. Millam, M. Klene, J. E. Knox, J. B. Cross, V. Bakken, C. Adamo, J. Jaramillo, R. Gomperts, R. E. Stratmann, O. Yazyev, A. J. Austin, R. Cammi, C. Pomelli, J. W. Ochterski, R. L. Martin, K. Morokuma, V. G. Zakrzewski, G. A. Voth, P. Salvador, J. J. Dannenberg, S. Dapprich, A. D. Daniels, O. Farkas, J. B. Foresman, J. V. Ortiz, J. Cioslowski, and D. J. Fox, Gaussian, Inc., Wallingford CT, 2013.
2. K. Masui, H. Nakanotani and C. Adachi, *Org. Electron.*, 2013, 14, 2721-2726.
3. Y. Yuan, X. Tang, X.-Y. Du, Y. Hu, Y.-J. Yu, Z.-Q. Jiang, L.-S. Liao and S.-T. Lee, Adv. Opt. Mater., 2019, 7, 1801536.
4. X. Li, Y. Z. Shi, K. Wang, M. Zhang, C. J. Zheng, D. M. Sun, G. L. Dai, X. C. Fan, D. Q. Wang, W. Liu, Y. Q. Li, J. Yu, X. M. Ou, C. Adachi and X. H. Zhang, *ACS Appl. Mater. Interfaces,* 2021, 13, 36089-36097
5. D. Sun, S. M. Suresh, D. Hall, M. Zhang, C. Si, D. B. Cordes, A. Slawin, Y. Olivier, X. Zhang and E. Zysman-Colman, *Mater. Chem. Front.*, 2020, 4, 2018-2022.
6. S. N. Zou, C. C. Peng, S. Y. Yang, Y. K. Qu, Y. J. Yu, X. Chen, Z. Q. Jiang and L. S. Liao, *Org Lett*, 2021, **23**, 958-962.
7. F. Huang, K. Wang, Y. Z. Shi, X. C. Fan, X. Zhang, J. Yu, C. S. Lee and X. H. Zhang, *ACS Appl Mater Interfaces*, 2021, **13**, 36089-36097.
8. H. Min, I. S. Park and T. Yasuda, *Angew Chem Int Ed Engl*, 2021, **60**, 7643-7648.
9. X. Qiu, G. Tian, C. Lin, Y. Pan, X. Ye, B. Wang, D. Ma, D. Hu, Y. Luo and Y. Ma, *Adv. Optical Mater. 2021, 9, 2001845.*
10. Y. Tsuchiya, Y. Ishikawa, S. H. Lee, X. K. Chen, J. L. Brédas, H. Nakanotani and C. Adachi, *Adv. Optical Mater. 2021, 9, 2002174.*
11. S. Y. Yang, S. N. Zou, F. C. Kong, X. J. Liao, Y. K. Qu, Z. Q. Feng, Y. X. Zheng, Z. Q. Jiang and L. S. Liao, *Chem Commun*, 2021, **57**, 11041-11044.
12. S. K. Surampudi, G. Nagarjuna, D. Okamoto, P. D. Chaudhuri and D. Venkataraman, J. Org. Chem., 2012, 77, 2074-2079.

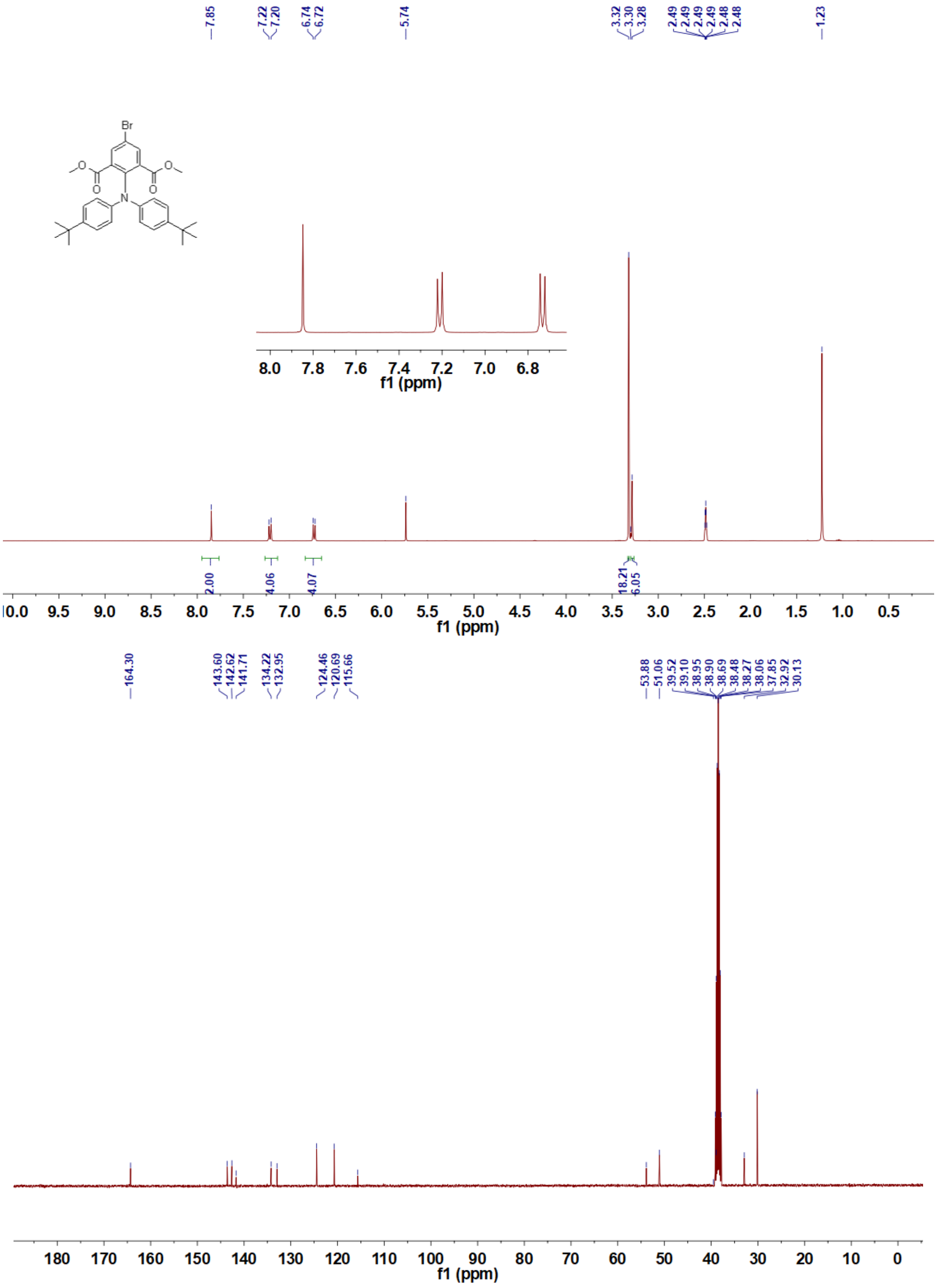

Fig. S12 ^{1}HNMR and ^{13}CNMR of Compound 4

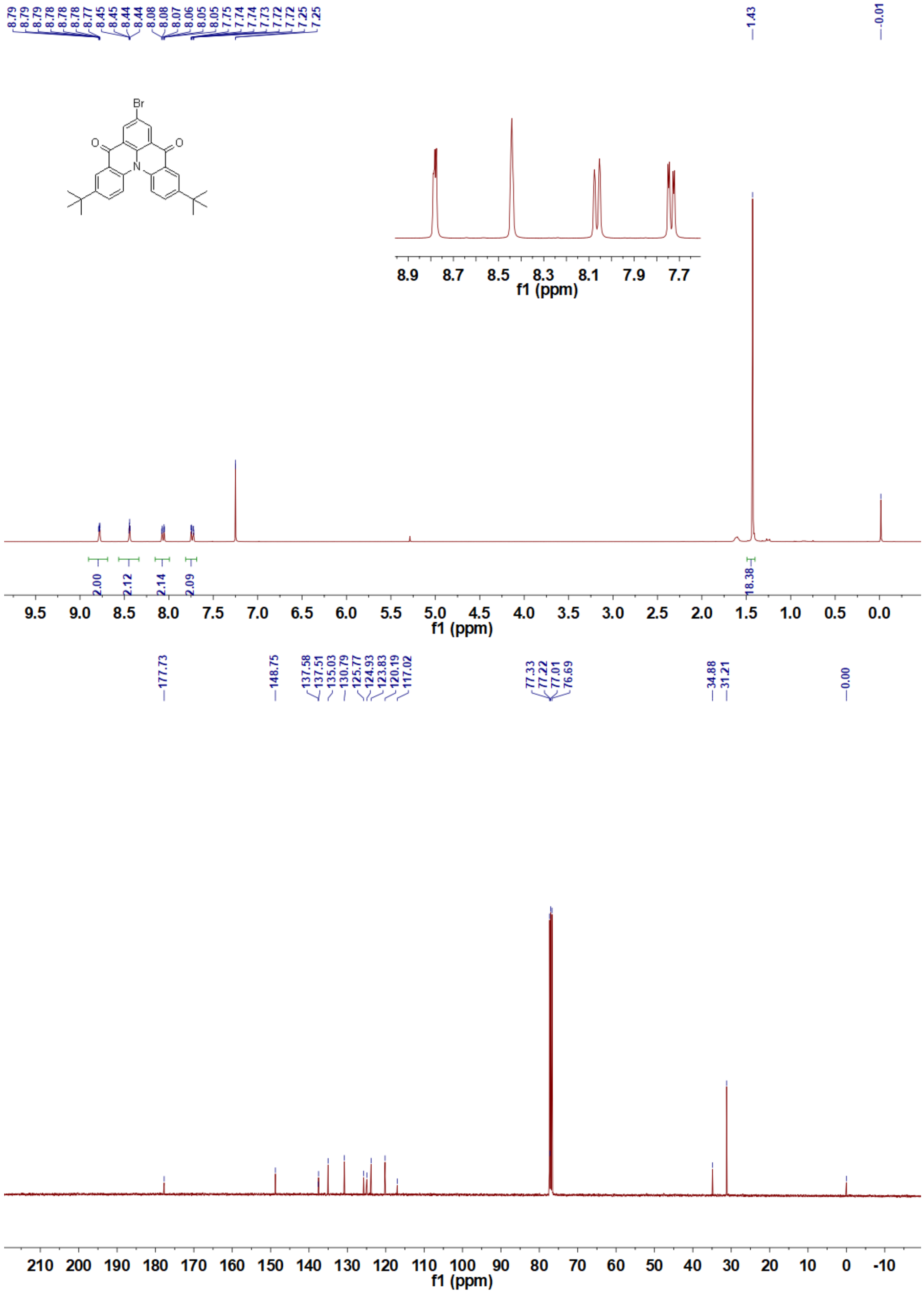

Fig. S13 ^{1}HNMR and ^{13}CNMR of Compound 6.

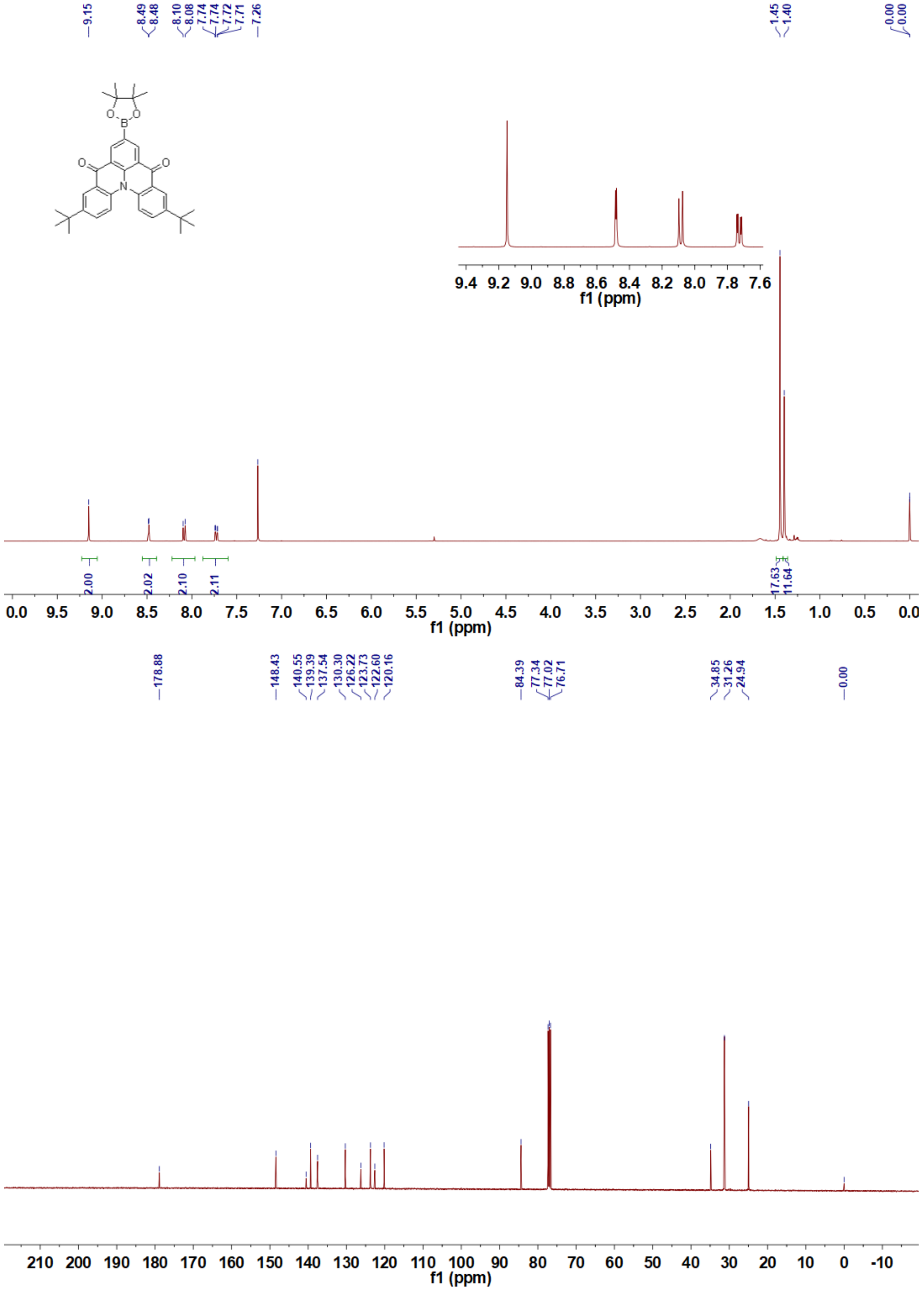

Fig. S14 ^{1}HNMR and ^{13}CNMR of Compound 7.

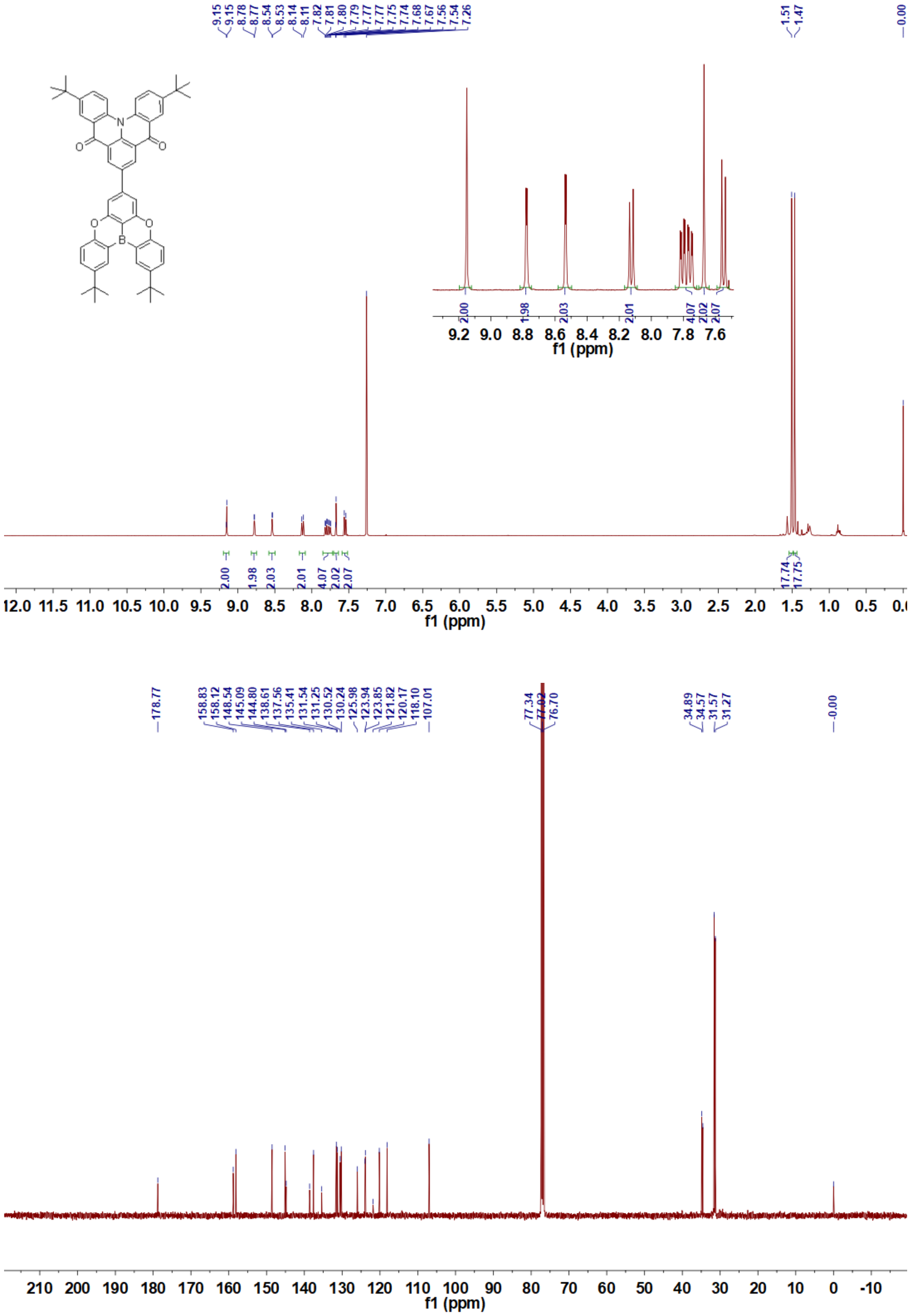

Fig. S15 ^{1}HNMR and ^{13}CNMR of BOQAO.

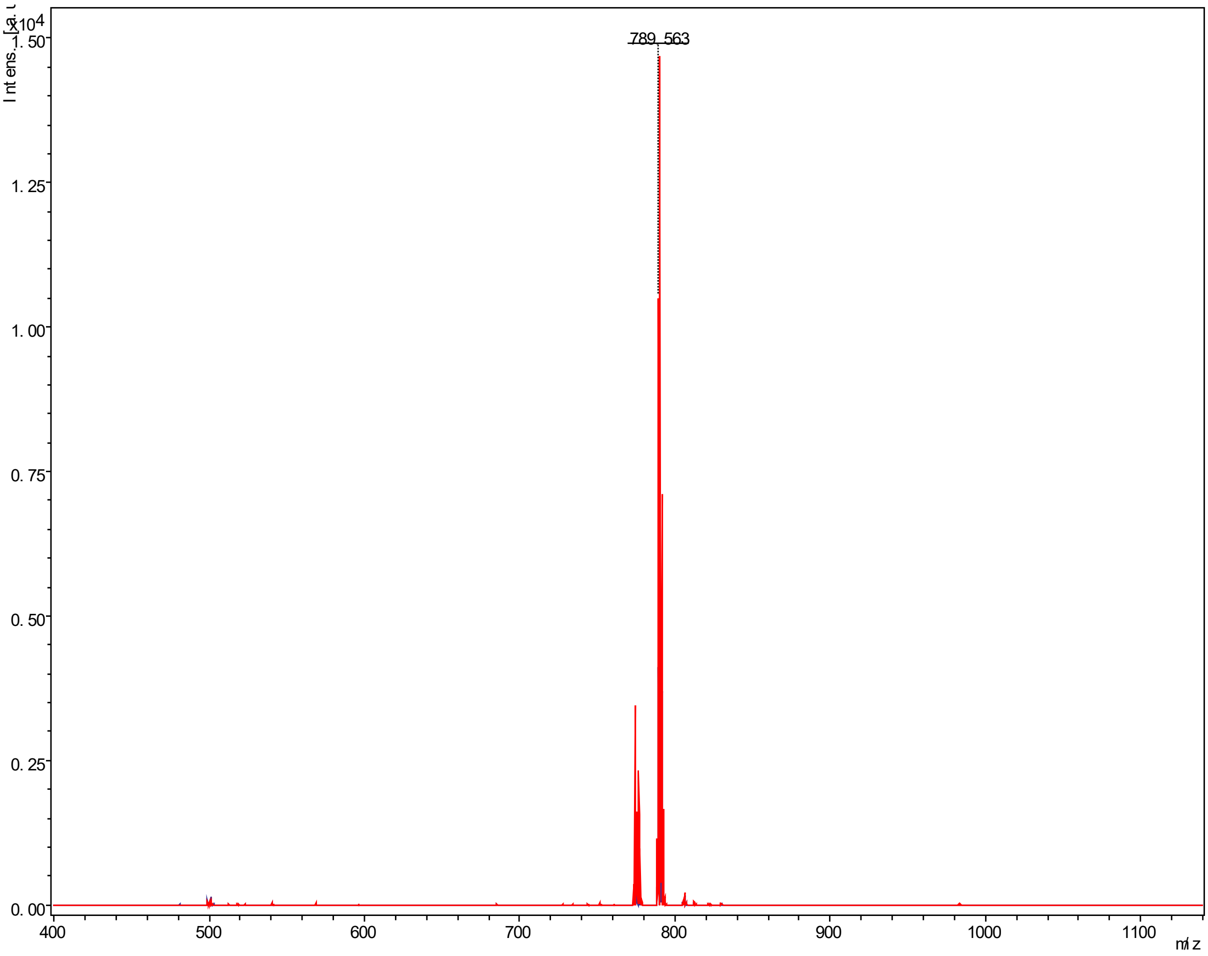

Fig. S16 MODI-TOF of BOQAO.